Identification of the G13 (cAMP-response-element-binding protein-related protein) gene product related to activating transcription factor 6 as a transcriptional activator of the mammalian unfolded protein response

Kyosuke HAZE*[1], Tetsuya OKADA†[1], Hiderou YOSHIDA*†, Hideki YANAGI*, Takashi YURA*, Manabu NEGISHI† and Kazutoshi MORI†[2]

*HSP Research Institute, Kyoto Research Park, 17 Chudoji-minami, Shimogyo-ku, Kyoto 600-8813, Japan, and †Graduate School of Biostudies, Kyoto University, 46-29 Yoshida-Shimoadachi, Sakyo-ku, Kyoto 606-8304, Japan

Eukaryotic cells control the levels of molecular chaperones and folding enzymes in the endoplasmic reticulum (ER) by a transcriptional induction process termed the unfolded protein response (UPR). The mammalian UPR is mediated by the *cis*-acting ER stress response element consisting of 19 nt ($CCAATN_9CCACG$), the CCACG part of which is considered to provide specificity. We recently identified the basic leucine zipper (bZIP) protein ATF6 as a mammalian UPR-specific transcription factor; ATF6 is activated by ER stress-induced proteolysis and binds directly to CCACG. Here we report that eukaryotic cells express another bZIP protein closely related to ATF6 in both structure and function. This protein encoded by the G13 (cAMP response element binding protein-related protein) gene is constitutively synthesized as a type II transmembrane glycoprotein anchored in the ER membrane and processed into a soluble form upon ER stress as occurs with ATF6. The proteolytic processing of ATF6 and the G13 gene product is accompanied by their relocation from the ER to the nucleus; their basic regions seem to function as a nuclear localization signal. Overexpression of the soluble form of the G13 product constitutively activates the UPR, whereas overexpression of a mutant lacking the activation domain exhibits a strong dominant-negative effect. Furthermore, the soluble forms of ATF6 and the G13 gene product are unable to bind to several point mutants of the *cis*-acting ER stress response element *in vitro* that hardly respond to ER stress *in vivo*. We thus concluded that the two related bZIP proteins are crucial transcriptional regulators of the mammalian UPR, and propose calling the ATF6 gene product ATF6α and the G13 gene product ATF6β.

Key words: chaperone, endoplasmic reticulum, nucleus, proteolysis, signalling.

INTRODUCTION

The endoplasmic reticulum (ER) contains multiple molecular chaperones and folding enzymes that assist and/or facilitate the folding and assembly of newly synthesized secretory and transmembrane proteins, and monitors the quality of proteins destined for the secretory pathway [1,2]. Although ER chaperones such as GRP78/BiP are expressed fairly abundantly under normal growth conditions, their levels are further increased to maintain homoeostasis of the ER under ER stress conditions that cause accumulation of unfolded proteins in the ER [3–6]. Induction of ER chaperones occurs at the level of transcription. Thus eukaryotic cells from yeast to man are equipped with an intracellular signalling pathway from the ER to the nucleus, termed the unfolded protein response (UPR) [7,8].

In mammals, the ER stress response element (ERSE) is the *cis*-acting element that is necessary and sufficient for the transcriptional induction of ER chaperones in response to ER stress [9,10]. The consensus sequence of ERSE is $CCAATN_9CCACG$. As the CCAAT part of ERSE is known to be a binding site for the general transcription factor NF-Y/CBF [11], the CCACG part 9 bp downstream is considered to confer specificity on the UPR and to explain why only a limited set of proteins are induced under ER stress conditions.

We isolated human basic leucine zipper (bZIP) protein ATF6 as a protein that would bind to the CCACG part of ERSE [9]. Subsequent analysis [12] revealed that ATF6 is synthesized as a 90 kDa transmembrane glycoprotein (p90ATF6) embedded in the ER under normal growth conditions and that p90ATF6 is converted into a 50 kDa soluble nuclear protein (p50ATF6) specifically in ER-stressed cells before the induction of GRP78. When overexpressed, p50ATF6-like ATF6 mutants were accumulated in the nucleus, leading to constitutively enhanced transcription of the endogenous GRP78 gene. We thus proposed that ATF6 is activated by ER stress-induced proteolysis [12]. It was shown previously that the CCAAT part of ERSE present in the GRP78 promoter is constitutively occupied [13] and we found that p50ATF6 binds directly to the CCACG part of ERSE only when the CCAAT part is bound to NF-Y [14]. On the basis of these findings, we proposed that the ER stress response factor (ERSF) binding to ERSE responsible for the mammalian UPR is a heterologous protein complex consisting of a constitutive component binding to the CCAAT part (NF-Y) and an inducible component binding to the CCACG part (ATF6). However, altered localization of endogenous ATF6 in response to ER stress has not been demonstrated.

Interestingly, mammalian cells express another bZIP protein that is closely related to ATF6 [15], which is encoded by the G13

Abbreviations used: AD, activation domain; bZIP, basic leucine zipper; CREB-RP, cAMP-response-element-binding protein-related protein; EMSA, electrophoretic mobility-shift assay; ER, endoplasmic reticulum; ERSE, endoplasmic reticulum stress response element; ERSF, endoplasmic reticulum stress response factor; GAL4BD, DNA-binding domain of yeast transcriptional activator Gal4p; HA, influenza virus haemagglutinin; NLS, nuclear localization signal; UPR, unfolded protein response.

[1] These authors contributed equally to this work.

[2] To whom correspondence should be addressed (e-mail kazumori@ip.media.kyoto-u.ac.jp).

[16] or cAMP-response-element-binding protein-related protein (CREB-RP) gene [17], although its function has remained unclear. We report here that the G13/CREB-RP gene product has properties very similar to those of ATF6 and thus participates in the mammalian UPR as a transcriptional activator. We therefore propose that the ATF6 gene product be called ATF6α and the G13/CREB-RP gene product ATF6β. We also visualized the relocation of the endogenous ATF6α and ATF6β from the ER to the nucleus in ER-stressed cells. A mutant ATF6β containing the bZIP domain but lacking the activation domain (AD) exhibited a strong dominant-negative effect on the UPR; transcriptional activities of various ERSE-like sequences were well correlated with their ATF6α and ATF6β binding activities, indicating their importance in the UPR.

MATERIALS AND METHODS

Cell culture and transfection

HeLa and HEK-293T cells were grown in Dulbecco's modified Eagle's medium supplemented with 10 % (v/v) fetal calf serum, 2 mM glutamine, 100 i.u./ml penicillin and 100 μg/ml streptomycin sulphate. Cells were maintained in an incubator under air/CO_2 (19:1) at 37 °C. Transfection of HeLa cells was performed by the standard calcium phosphate method [18] essentially as described previously [12]. HEK-293T cells were transfected with LIPOFECTAMINE 2000 reagent (Gibco BRL, Rockville, MD, U.S.A.) in accordance with the manufacturer's instructions.

Plasmid construction

Recombinant DNA techniques were performed by standard procedures [18]. Plasmids for expression of ATF6α and ATF6β were constructed on the basis of the mammalian expression vector pcDNA3.1(+) (Invitrogen, Carlsbad, CA, U.S.A.), pCGN [19], pMYC-CMV (Clontech, Palo Alto, CA, U.S.A.) or pBIND (Promega, Madison, WI, U.S.A.). pcDNA-ATF6β (703), pcDNA-ATF6α (670) and pCGN-ATF6α (670) were identical with pcDNA-CREB-RP [9], pcDNA-ATF6 [9] and pCGN-ATF6 (670) [12] respectively. [The numbers such as (703) and (670) indicates the length of the ATF6 protein encoded by the plasmid; thus pcDNA-ATF6β (703) expresses the full-length ATF6β protein (amino acids 1–703); similarly pcDNA-ATF6α (670) expresses the full-length ATF6α protein (amino acids 1–670).] Various subregions of ATF6α or ATF6β were amplified by PCR together with a stop codon and inserted into appropriate restriction enzyme sites in expression vectors after their sequences had been confirmed.

Immunoblotting and indirect immunofluorescence

Rabbit anti-ATF6α and anti-ATF6β antibodies raised against the N-terminal region of ATF6α (residues 6–307) and that of ATF6β (residues 1–307) respectively were purified as described previously [12,14]. Rabbit anti-[influenza virus haemagglutinin (HA) epitope] polyclonal antibody (Y-11) and mouse anti-(c-Myc epitope) monoclonal antibody (9E10) were obtained from Santa Cruz Biotechnology (Santa Cruz, CA, U.S.A.). Mouse anti-KDEL monoclonal antibody (clone 10C3) was obtained from StressGen Biotechnologies (Victoria, British Columbia, Canada).

For immunoblotting, HeLa cells cultured in 60 mm dishes were washed with PBS, scraped with a rubber 'policeman' and lysed in 50 μl of Laemmli SDS sample buffer. After being boiled for 5 min, 5 μl aliquots of each sample were subjected to SDS/PAGE [7.5 % (w/v) gel] and analysed by the standard procedure [18] with an enhanced chemiluminescence Western blotting detection system kit (Amersham Pharmacia Biotech, Little Chalfont, Bucks., U.K.). For immunofluorescence, HeLa cells cultured on slide glasses were fixed, permeabilized and stained as described previously [12].

Northern blot hybridization

Total RNA was extracted from HeLa cells or HEK-293T cells by the acid guanidinium/phenol/chloroform method with Isogen obtained from Nippon Gene (Tokyo, Japan). Aliquots of 10 μg were subjected to electrophoresis on 1 % (w/v) agarose gels containing 2.2 M formaldehyde and analysed by the standard procedure [18].

Luciferase assays

HeLa cells cultured in 96-well plates were transfected with reporter plasmid (0.2 μg) carrying the firefly luciferase gene and reference plasmid pRL-SV40 (in which SV40 stands for simian virus 40) (0.02 μg) carrying the *Renilla* luciferase gene under the control of the SV40 enhancer and promoter (Promega) in the presence or absence of effector plasmid (0.2 μg). After 48 h, cells were lysed in 20 μl of passive lysis buffer (Promega). Firefly luciferase and *Renilla* luciferase activities were measured with 5 μl of cell lysate by using the Dual-Luciferase Reporter Assay System (Promega) and a Luminoskan luminometer (Labsystems, Helsinki, Finland). Relative luciferase activity was defined as the ratio of firefly luciferase activity to *Renilla* luciferase activity.

Electrophoretic mobility-shift assay (EMSA)

Recombinant NF-Y trimer was prepared as described previously [14]. ATF6α (373) and ATF6β (392) were translated *in vitro* with the TNT T7 quick coupled transcription/translation system (Promega). EMSA was performed essentially as described previously [14] except that samples were loaded on non-denaturing gradient (5–20 %, w/v) polyacrylamide gels and electrophoresed at 4 °C at 200 V for 150 min in 0.5 × TBE buffer, consisting of 45 mM Tris/borate and 1 mM EDTA.

RESULTS

ATF6β is synthesized as a type II transmembrane glycoprotein in the ER and subjected to proteolysis in response to ER stress

ATF6β (the G13/CREB-RP gene product) shows significant sequence similarity to ATF6α (the ATF6 gene product), not only in the bZIP region but also in the N-terminal and C-terminal regions (Figure 1A), as described previously [15]. Most importantly, ATF6β contains an internal hydrophobic stretch consisting of 21 residues near the centre of the molecule, suggesting that ATF6β is synthesized as a type II transmembrane protein, as is ATF6α. This notion was firmly supported by the results of biochemical analysis conducted as reported previously for ATF6α [12]; that is, subcellular fractionation followed by differential solubilization and topological analysis (results not shown). Immunoblotting analysis with anti-ATF6β antibody raised and purified as described in the Materials and methods section revealed that ATF6β was synthesized constitutively as a protein of 110 kDa (designated p110ATF6β) in HeLa cells (Figure 1B, lane 2). p110ATF6β was glycosylated, because treatment with endoglycosidase H decreased its apparent molecular mass on SDS/PAGE (Figure 1B, lane 3), resulting in migration at the same position as that of full-length ATF6β translated *in vitro* (lane 1); the luminal domain of ATF6β contained five potential glycosylation sites, as shown in Figure

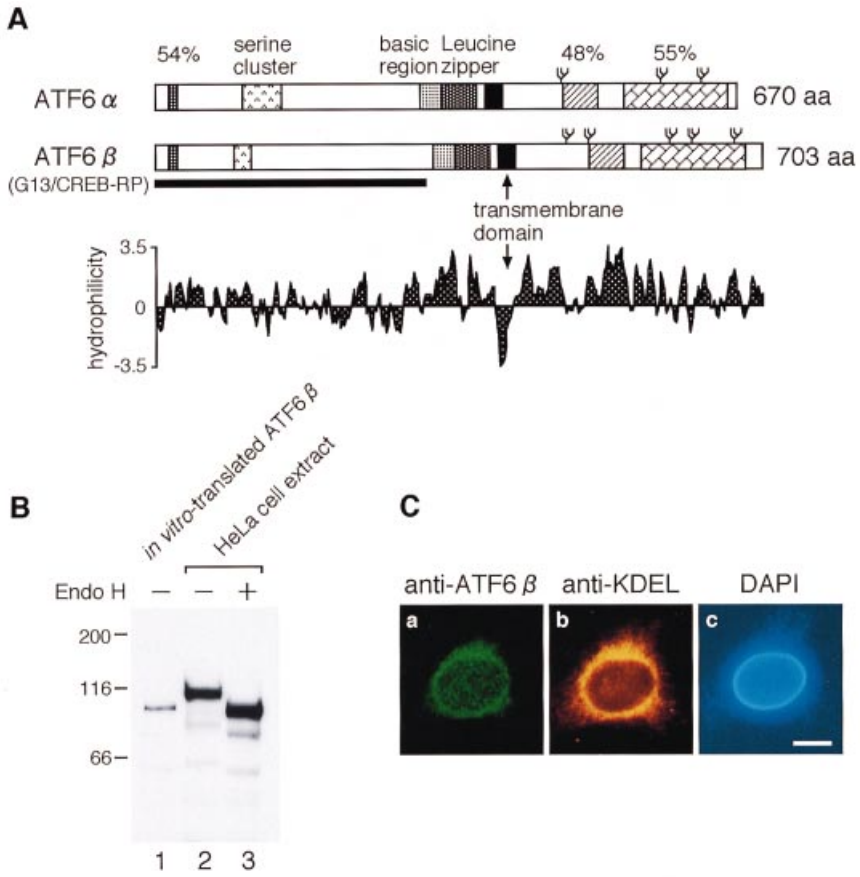

Figure 1 Anchoring of ATF6β in the ER membrane by an internal hydrophobic stretch

(**A**) Schematic structures of ATF6α (the ATF6 gene product) and ATF6β (the G13/CREB-RP gene product). The positions of the serine cluster, basic region, leucine zipper and transmembrane domain are indicated. The regions showing significant similarity are marked by boxes with percentage identities as previously reported [15]. The thick line below the ATF6β sequence denotes the region used to raise the antibody against ATF6β. The potential N-glycosylation sites are shown schematically. The hydropathy index was calculated by the method of Kyte and Doolittle [29]. Abbreviation: aa, residues. (**B**) Glycosylation analysis. Aliquots of 2.5 μg of proteins in the 1000 ***g*** supernatant fraction prepared from unstressed HeLa cells were digested with (lane 3) or without (lane 2) endoglycosidase H (Endo H), essentially as described previously [12]. Samples as well as full-length ATF6β translated *in vitro* (lane 1) were subjected to SDS/PAGE and analysed by immunoblotting with anti-ATF6β antibody. The positions of prestained SDS/PAGE molecular mass standards (Bio-Rad, Hercules, CA, U.S.A.) are indicated (in kDa). (**C**) Indirect immunofluorescence analysis. Unstressed HeLa cells were fixed and stained with anti-ATF6β antibody (**a**), anti-KDEL antibody (**b**) or 4,6-diamidino-2-phenylindole (**c**). Scale bar, 10 μm.

1(A). When HeLa cells were stained with anti-ATF6β antibody, fine reticular structures were observed (Figure 1C, panel a) and the staining pattern was almost indistinguishable from that obtained with anti-KDEL antibody (Figure 1C, panel b), which recognizes two major ER chaperones GRP78 and GRP94 in HeLa cells. We therefore concluded that ATF6β is synthesized constitutively as a type II transmembrane glycoprotein anchored in the ER membrane, similarly to ATF6α. Northern blot hybridization analysis indicated that ATF6α mRNA and ATF6β mRNA were expressed ubiquitously (Figure 2), which is consistent with previous reports [15–17]. Quantitative immunoblotting analysis revealed that ATF6β was expressed as abundantly as ATF6α in HeLa cells (results not shown).

When HeLa cells were treated with ER stress-inducing reagents, such as thapsigargin (an inhibitor of the ER Ca^{2+} ATPase [20]) and tunicamycin (an inhibitor of protein N-glycosylation [3,4]), proteolytic processing of ATF6α was induced; the p90ATF6α level decreased and p50ATF6α appeared before the induction of GRP78 (Figures 3A and 3B, lower panels) as we reported previously [12]. Similarly, the p110ATF6β level decreased and instead a new band of approx. 60 kDa (designated p60ATF6β) was detected in HeLa cells treated with thapsigargin (Figure 3A, upper panel) or tunicamycin (Figure 3B, upper panel), indicating that ATF6β also underwent proteolysis in response to ER stress. Interestingly, the time course of the appearance of p60ATF6β was quite similar to that of p50ATF6α in thapsigargin-treated cells (Figure 3A), whereas p60ATF6β was detected in a sustained manner in comparison with the transient detection of p50ATF6α in tunicamycin-treated cells (Figure 3B). These results suggest that the ER stress-induced proteolysis of ATF6β might be regulated differently from that of ATF6α under certain conditions of ER stress.

p60ATF6β liberated from the ER membrane translocates into the nucleus

We examined the consequences of the conversion of p110ATF6β into p60ATF6β. Fractionation analysis revealed that p60ATF6β was recovered in the nuclear fraction as a soluble protein, in contrast with p110ATF6β anchored in the ER membrane (results not shown), suggesting that ER stress-induced proteolysis alters the subcellular localization of ATF6β. We had

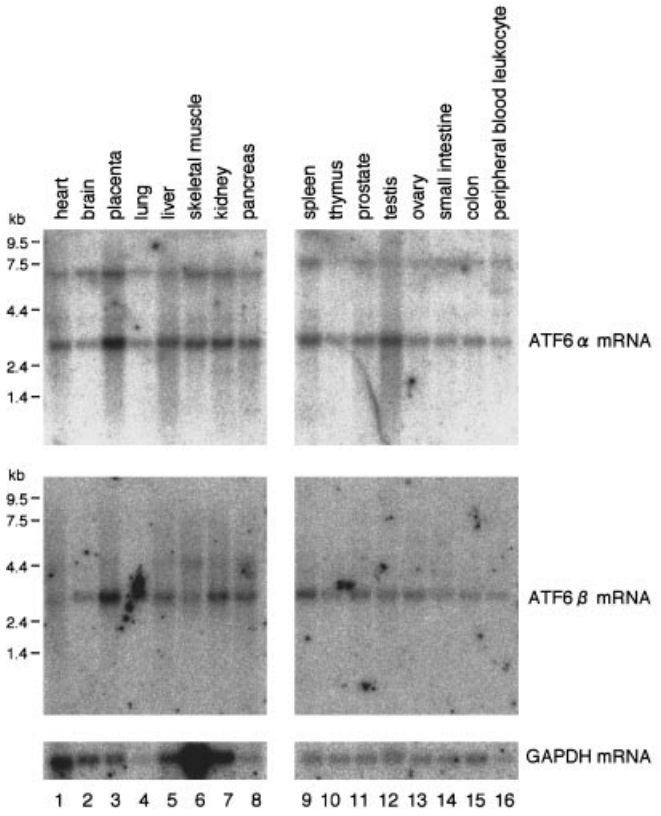

Figure 2 Tissue distribution of ATF6α mRNA and ATF6β mRNA

A nylon membrane, to which aliquots of 2 μg of poly(A)$^+$ RNA prepared from various human tissues had been blotted as indicated (Clontech), was hybridized with ^{32}P-labelled cDNA probe specific for human ATF6α (top panels), human ATF6β (middle panels) or human GAPDH (bottom panels). The positions of RNA size markers are also shown.

previously failed to visualize the relocation of endogenous ATF6α from the ER to the nucleus in response to ER stress [12] because the amounts of p50ATF6α produced were insufficient for detection by immunofluorescence analysis when cells were treated with any of the three ER stress inducers tested, i.e. thapsigargin, tunicamycin and A23187 (a calcium ionophore) [3]. This was also true for ATF6β (results not shown). We therefore tested another inducer, dithiothreitol, which causes the malfolding of proteins in the ER directly by disrupting disulphide bonds, to determine the localization of both endogenous ATF6α and ATF6β.

Treatment of HeLa cells with 0.3 mM dithiothreitol rapidly triggered proteolysis of ATF6α (within 30 min) but the amounts of p50ATF6α produced were still too low for immunofluorescence analysis (Figure 4A), in a similar manner to those produced by thapsigargin or tunicamycin treatment (see Figure 3). However, we found that this rapid processing of ATF6α became much more extensive in cells treated with higher concentrations of dithiothreitol, in a dose-dependent manner. Approximately half of p90ATF6α was converted into p50ATF6α 0.5 h after treatment with 1.0 mM dithiothreitol, and all had been converted after 1 h (Figure 4A and Figure 4B, lane 2). p110ATF6β was also converted into p60ATF6β rapidly and extensively in cells treated with 1.0 mM dithiothreitol (Figure 4B, lane 2). These rapid conversions were immediately followed by the induction of GRP78 mRNA, a major target of the mammalian UPR; the level of GRP78 mRNA was already elevated at 1 h and peaked at 4 h. Accordingly, the increase in the level of GRP78 was observed as early as 4 h.

Under these conditions, localization of ATF6α and ATF6β was determined by indirect immunofluorescence analysis. As reported previously [12], ATF6α was present in perinuclear structures of unstressed cells (Figure 5A, panel a) and the staining pattern overlapped with that obtained with anti-KDEL antibody (panel b). In contrast, both nucleus and ER-like structures were stained with anti-ATF6α antibody when cells were treated with 1.0 mM dithiothreitol for 0.5 h (Figure 5A, panel d), which was consistent with the presence of almost equal amounts of p50ATF6α and p90ATF6α (see Figure 4A). Moreover, only the nucleus was stained after treatment of cells for 1 h (Figure 5A, panel g), in which only p50ATF6α was detected (see Figure 4A). Similarly, relocation of endogenous ATF6β was visualized in dithiothreitol-treated HeLa cells (Figure 5B). Thus ATF6α and ATF6β did indeed alter their subcellular localization from the ER to the nucleus when processed in response to ER stress.

Basic region functions as nuclear localization signal (NLS)

The above results indicated that both ATF6α and ATF6β translocate into the nucleus once liberated from the ER membrane. This prompted us to identify the region(s) important for nuclear localization of p50ATF6α and p60ATF6β. When a cDNA encoding full-length ATF6β was transfected into HeLa cells, ATF6β (703) was localized in ER-like perinuclear structures (Figure 6i) as expected. In contrast, a C-terminal deletion mutant of ATF6β, ATF6β (392), lacking the luminal and transmembrane domains (see Figure 6, upper panel), was accumulated in the nucleus in transfected cells (Figure 6k). It should be noted that when translated *in vitro*, ATF6β (392) migrated at the same position as p60ATF6β on SDS/PAGE (see Figure 3). These results strongly suggested that p60ATF6β represented the entire cytoplasmic region of ATF6β. We therefore used ATF6β (392) as a representative of p60ATF6β in the following experiments.

As reported previously [12], ATF6α (373) lacking the luminal and transmembrane domains was accumulated in the nucleus (Figure 6c), whereas full-length ATF6α, ATF6α (670), was localized in ER-like structures (Figure 6a). Thus ATF6α (373) and ATF6β (392) must possess NLS. We therefore constructed further C-terminal deletion mutants of ATF6α and ATF6β and determined their localization in transfected cells. Deletion of the leucine zipper from ATF6α (373) or ATF6β (392) did not significantly affect localization (Figures 6e and 6m). In marked contrast, both ATF6α (302) and ATF6β (310) lacking the basic region as well as the leucine zipper were distributed throughout the cell (Figures 6g and 6o), indicating the indispensability of the basic region for the nuclear localization of ATF6α and ATF6β.

p60ATF6β binds directly to ERSE in the presence of NF-Y

Next we examined whether the p60ATF6β-like mutant ATF6β (392) could bind to ERSE directly. Synthetic double-stranded oligonucleotides of 41 bp encoding ERSE1 and its surrounding sequences present in the human GRP78 promoter were used as probes for EMSA after being labelled with ^{32}P. To elucidate the specificity, two regions indispensable for the function of ERSE were mutated separately or simultaneously. For convenience, wild-type and mutant sequences are denoted as C (complete) and M (mutant) respectively. Thus ERSE-CC indicates the perfect consensus sequence, CCAATN$_9$CCACG, whereas ERSE-CM, ERSE-MC and ERSE-MM indicate the mutated sequences, CCAATN$_9$gatgt, gactaN$_9$CCACG and gactaN$_9$gatgt respectively, as indicated by lower-case letters.

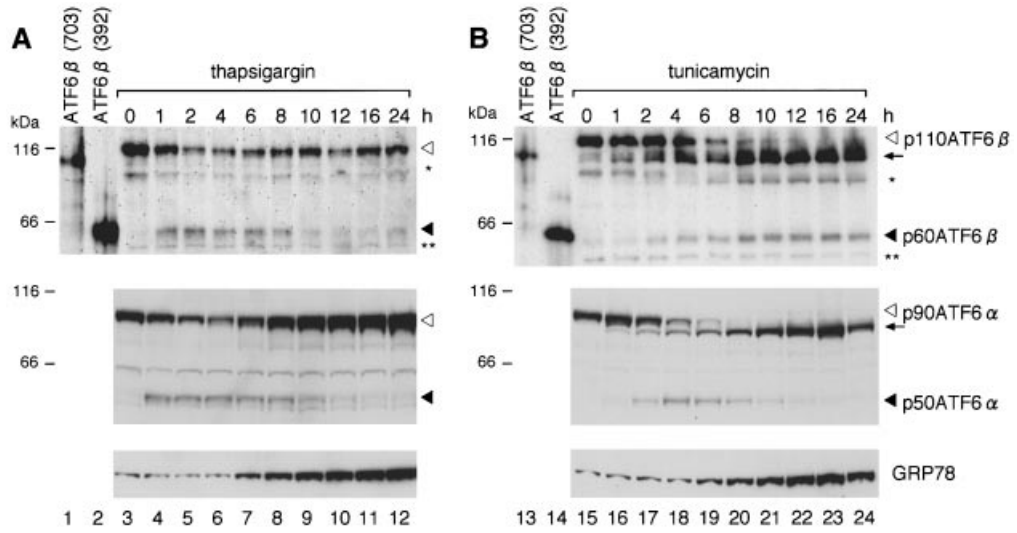

Figure 3 Effects of treatment of HeLa cells with thapsigargin (A) and tunicamycin (B) on the processing of ATF6α and ATF6β

HeLa cells cultured in 60 mm dishes until 60% confluence were incubated in the presence of 300 nM thapsigargin (**A**) or 2 μg/ml tunicamycin (**B**) for the indicated periods. The cells were lysed directly in 50 μl of Laemmli SDS sample buffer and boiled for 5 min. Aliquots (5 μl) of the samples were subjected to SDS/PAGE and analysed by immunoblotting with anti-ATF6α antibody, anti-ATF6β antibody or anti-KDEL antibody, which recognizes GRP78. Full-length ATF6β, ATF6β (703), and a C-terminal deletion mutant of ATF6β, ATF6β (392), all translated *in vitro*, were analysed similarly with anti-ATF6β antibody. The positions of p110ATF6β, p60ATF6β, p90ATF6α and p50ATF6α are indicated by arrowheads. The arrows denote unglycosylated forms of p110ATF6β or p90ATF6α. The bands marked by asterisks seemed to be degradation products of p110ATF6β because their intensity increased during storage of samples. The band migrating faster than p60ATF6β and marked by double asterisks was present at all time points and was therefore probably non-specific. The positions of molecular mass markers are indicated (in kDa) at the left.

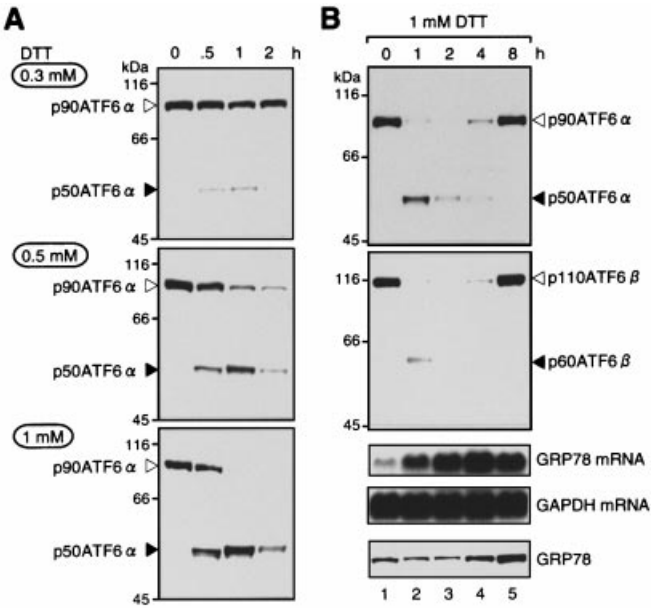

Figure 4 Rapid and extensive processing of ATF6α and ATF6β in dithiothreitol-treated HeLa cells

(**A**) Effects of treatment with dithiothreitol on the processing of ATF6α. HeLa cells cultured in 60 mm dishes until 70% confluence were incubated in the presence of various concentrations of dithiothreitol for the indicated periods. Cell lysates were prepared and analysed by immunoblotting with anti-ATF6α antibody as described in the legend to Figure 3. The positions of p90ATF6α and p50ATF6α are marked by the open and filled arrowheads respectively. (**B**) Correlation of the processing of ATF6α/β with the induction of GRP78. HeLa cells cultured in 60 mm dishes until 80% confluence were incubated in the presence of 1 mM dithiothreitol for the indicated periods. Cell lysates were prepared and analysed by immunoblotting as described in the legend to Figure 3. Total RNA was also extracted and analysed by Northern blot hybridization with radiolabelled probes specific for GRP78 or GAPDH. The positions of molecular mass markers are indicated (in kDa) at the left of each panel.

Recombinant NF-Y recognizing the CCAAT sequence bound to ERSE-CC and ERSE-CM, resulting in the formation of a protein–DNA complex designated complex I (Figure 7A, lanes 2 and 8), as expected from the results reported previously [11]. Although ATF6β (392) translated *in vitro* did not bind by itself to ERSE-CC (Figure 7A, lane 3), ATF6β (392) bound to ERSE-CC in the presence of NF-Y, giving rise to the formation of a novel protein–DNA complex designated complex II (lane 4). Importantly, the formation of complex II was blocked by pretreatment of the mixture of NF-Y and ATF6β (392) with anti-ATF6β antibody (Figure 7A, lane 6) but not with anti-ATF6α antibody (lane 5) before incubation with ^{32}P-labelled ERSE-CC. Intactness of the CCACG part was necessary for the binding of ATF6β (392) to ERSE because complex II was not formed even in the presence of NF-Y when ATF6β (392) was incubated with ^{32}P-labelled ERSE-CM (Figure 7A, lane 9). Furthermore, complex II formation was completely competed for by a 100-fold molar excess of ERSE-CC (Figure 7B, lane 11) and ERSE-CM (lane 12), to which NF-Y can bind, but not by ERSE-MC (lane 13) or ERSE-MM (lane 14), to which NF-Y cannot bind, indicating that the binding of ATF6β (392) to ERSE depends absolutely on the prebinding of NF-Y to ERSE. Thus the DNA-binding properties of ATF6β (392) were indistinguishable from those of ATF6α (373), which we had characterized previously [14]. These results implied that p60ATF6β translocated into the nucleus could modulate cellular UPR activity via direct binding to the CCACG part of ERSE.

p60ATF6β activates the transcription of mammalian UPR target genes

We reported previously that the overexpression of full-length ATF6β, ATF6β (703), inhibited the activation by ER stress of various promoters of ER chaperone genes [9] as reproduced in Figure 7(C) (compare the filled column in line 1 with that in line

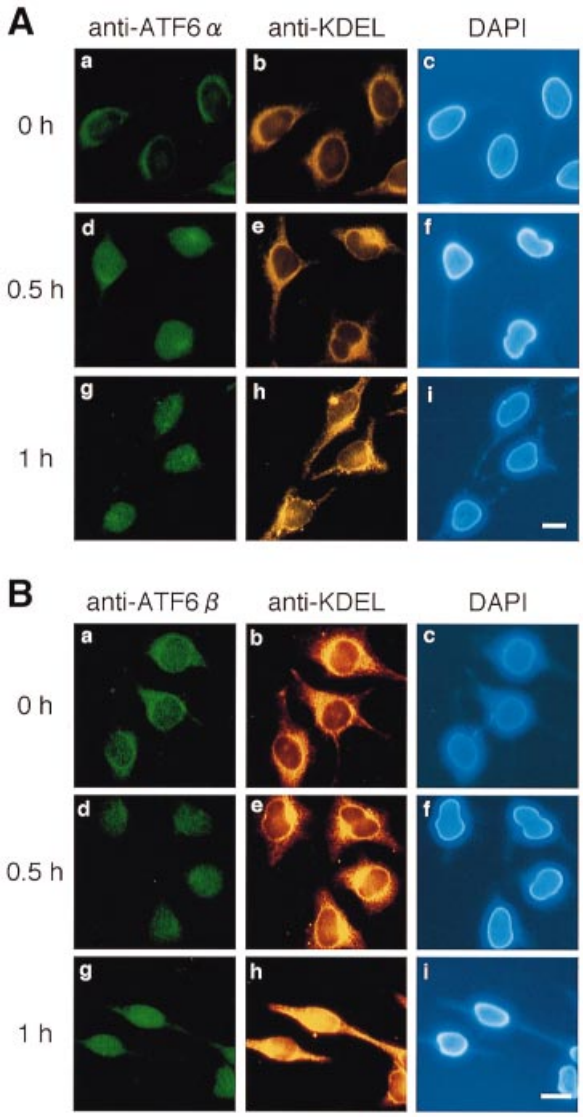

Figure 5 Indirect immunofluorescence analysis of HeLa cells treated with dithiothreitol

(**A**) Localization of ATF6α. HeLa cells untreated (**a**–**c**) or treated with 1.0 mM dithiothreitol for 0.5 h (**d**–**f**) or 1 h (**g**–**i**) were stained with anti-ATF6α antibody (**a**, **d**, **g**), anti-KDEL antibody (**b**, **e**, **h**) or 4,6-diamidino-2-phenylindole (**c**, **f**, **i**). Scale bar, 10 μm. (**B**) Localization of ATF6β. Indirect immunofluorescence analysis was performed as in (**A**) with anti-ATF6β antibody instead of anti-ATF6α antibody.

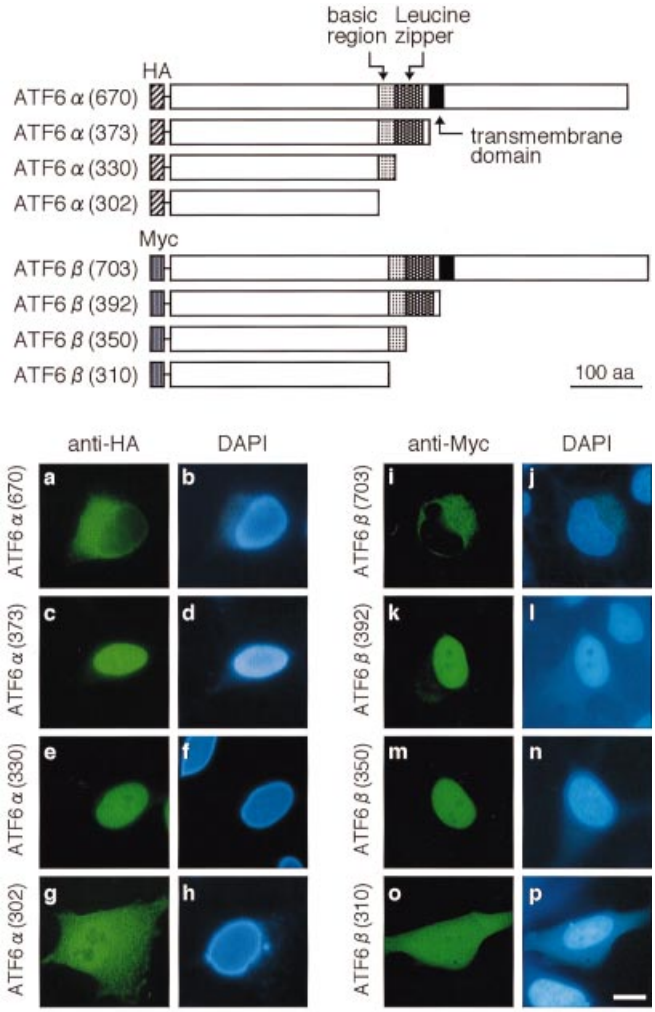

Figure 6 Effects of C-terminal deletions on localization of ATF6α and ATF6β

Schematic structures of full-length and various C-terminal deletion mutants of ATF6α and ATF6β cloned into the mammalian expression vectors pCGN and pMYC-CMV respectively are shown at the top. Expressed ATF6α and ATF6β were tagged with HA and Myc epitopes respectively at the N-terminus as indicated. The positions of the basic region, leucine zipper and transmembrane domain are marked. Abbreviation: aa, residues. HeLa cells transiently transfected with each of the indicated expression plasmids were stained with anti-HA epitope antibody (**a**, **c**, **e**, **g**), anti-Myc epitope antibody (**i**, **k**, **m**, **o**) or 4,6-diamidino-2-phenylindole (**b**, **d**, **f**, **h**, **j**, **l**, **n**, **p**). Scale bar, 10 μm.

3). This observation suggested that ATF6β might function as a negative regulator of the mammalian UPR [9]. Unexpectedly, however, overexpression of the p60ATF6β-like mutant, ATF6β (392), resulted in the constitutive activation of the GRP78 promoter (Figure 7C; compare the open column in line 1 with that in line 4) as for the p50ATF6α-like mutant, ATF6α (373) (open column in line 2). These stimulatory effects on the UPR were dependent on the ERSE because the elimination of three functional ERSEs from the GRP78 promoter abolished the enhancement (Figure 7C, lines 5–8). The level of endogenous GRP78 was indeed elevated in cells overexpressing ATF6β (392) as in cells overexpressing ATF6α (373) (Figure 7D). These results indicated that ATF6β was functioning as a transcriptional activator of the mammalian UPR. The reason why the over-expression of full-length ATF6β reproducibly exerted a negative effect on the UPR is not yet clear.

Mutant of p60ATF6β exhibits a dominant-negative effect on the UPR

We next determined whether p60ATF6β contained an AD that could be transplanted to unrelated DNA-binding proteins such as the DNA-binding domain of yeast transcriptional activator Gal4p (GAL4BD). Various subregions of ATF6β were fused in frame to GAL4BD and their transcriptional activities were determined by co-transfection with the reporter plasmid pG5luc containing five GAL4BD-binding sites upstream of a minimum promoter–firefly luciferase fusion gene. As expected from the results shown in Figures 7(C) and 7(D), GAL4BD fused with

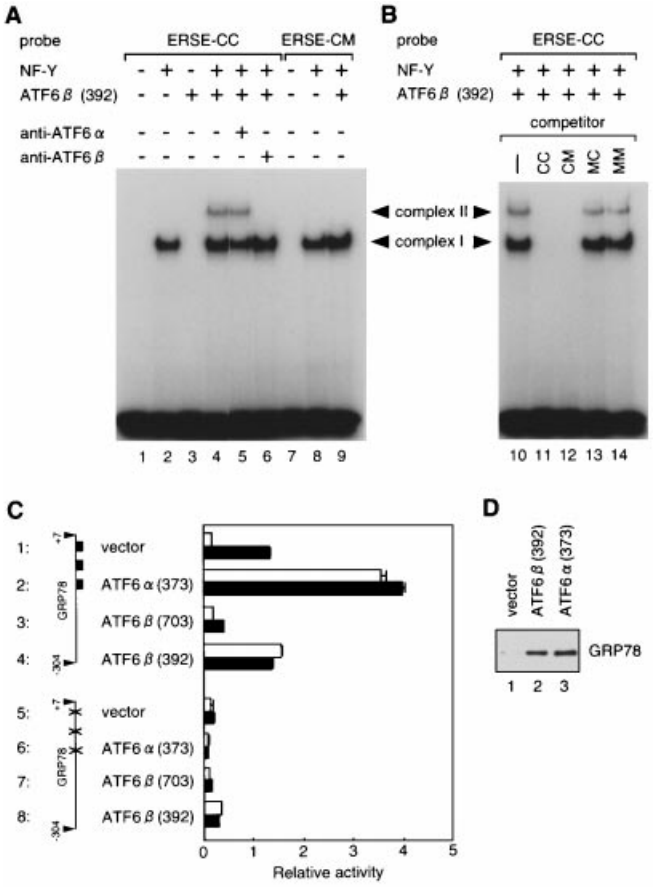

Figure 7 Identification of p60ATF6β as a transcriptional activator

(**A**) Direct binding of p60ATF6β to ERSE in the presence of NF-Y. ^{32}P-labelled oligonucleotide probe ERSE-CC containing CCAATN$_9$CCACG (lanes 1–6) or ERSE-CM containing CCAATN$_9$gatgt (lanes 7–9) was incubated with ATF6β (392) translated *in vitro* in the presence (+) or absence (−) of recombinant NF-Y. EMSA was performed as described in the Materials and methods section. The positions of complex I and complex II are indicated. A mixture of ATF6β (392) translated *in vitro* and recombinant NF-Y was treated with anti-ATF6α antibody (lane 5) or ATF6β antibody (lane 6) before incubation with ^{32}P-labelled ERSE-CC. (**B**) Competition assay. The specific binding of ATF6β (392) translated *in vitro* and recombinant NF-Y to ^{32}P-labelled ERSE-CC was competed for by a 100-fold molar excess of unlabelled oligonucleotides as indicated. ERSE-MC and ERSE-MM contained gactaN$_9$CCACG and gactaN$_9$gatgt respectively. (**C**) Effects of overexpression of ATF6β (392) on ERSE-mediated transcription. HeLa cells were transfected with pcDNA3.1(+) alone (vector), with pcDNA-ATF6α (373), with pcDNA-ATF6β (703) or with pcDNA-ATF6β (392) together with the reporter plasmid carrying the human GRP78 promoter (−304 to +7; numbers indicate nucleotide positions from the transcription start site) fused to the firefly luciferase gene. The GRP78 promoter used in lines 1–4 contained three functional ERSEs, whereas that in lines 5–8 carried mutated and thus inactive ERSEs as drawn schematically. Transfected cells were incubated either in the absence (open columns) or presence (filled columns) of 2 μg/ml tunicamycin for 16 h before harvesting. Relative luciferase activities were determined; results are means ± S.D. for four independent experiments. (**D**) Effects of overexpression of ATF6β (392) on the level of endogenous GRP78. HeLa cells cultured in 60 mm dishes were transfected with 10 μg of vector alone, 10 μg of pcDNA-ATF6β (392) or 10 μg of pcDNA-ATF6α (373). At 48 h after transfection, cell lysates were prepared and analysed by immunoblotting with anti-KDEL antibody as described in the legend to Figure 3.

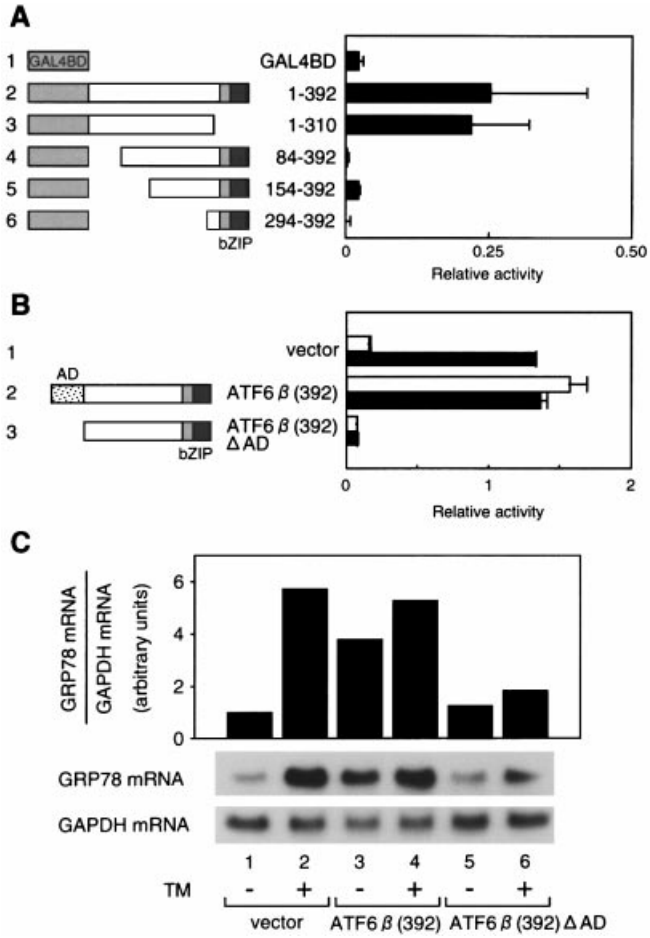

Figure 8 Construction of dominant-negative mutant of ATF6β

(**A**) Transactivator activity of ATF6β. Various subregions of ATF6β were fused in frame to GAL4BD in the mammalian expression vector pBIND as shown schematically at the left. Numbers indicate amino acid positions from the N-terminus. HeLa cells were transfected with each of the indicated expression plasmids together with the reporter plasmid pG5luc, which contained five GAL4BD-binding sites upstream of the firefly luciferase gene. The relative activities of luciferase constitutively expressed in transfected cells were determined and are presented as means ± S.D. for four independent experiments. (**B**) Effects of overexpressing ATF6β (392) ΔAD on ERSE-mediated transcription. Structures of the plasmid constructs used are shown schematically at the left. HeLa cells were transfected with vector alone, with pcDNA-ATF6β (392) or with pcDNA-ATF6β (392) ΔAD together with the reporter plasmid carrying the human GRP78 promoter with three functional ERSEs upstream of the firefly luciferase gene. Transfected cells were treated with (filled columns) or without (open columns) 2 μg/ml tunicamycin for 16 h before harvesting. Relative luciferase activities were determined; results are means ± S.D. for four independent experiments. (**C**) Effects of overexpressing ATF6β (392) ΔAD on the induction of GRP78 mRNA. HEK-293T cells in 60 mm dishes were transfected with 10 μg of vector alone, 10 μg of pcDNA-ATF6β (392) or 10 μg of pcDNA-ATF6β (392) ΔAD. At 24 h after transfection, cells were treated with (+) or without (−) 2 μg/ml tunicamycin (TM) for 8 h. Total RNA was prepared and analysed by Northern blot hybridization with radiolabelled probes specific for GRP78 or GAPDH.

residues 1–392 (Figure 8A, line 2) or 1–310 (line 3) of ATF6β activated transcription markedly in comparison with GAL4BD alone (line 1).

Because deletion analysis revealed that the N-terminal 83 residues of ATF6β were required for its transactivator activity (Figure 8A, line 4), we constructed a mutant of p60ATF6β lacking this region, ATF6β (392) ΔAD (residues 84–392), and examined the effects of its overexpression on the UPR. The overexpression of ATF6β (392), used as a control, constitutively activated the GRP78 promoter including three functional ERSEs (Figure 8B, line 2). In marked contrast, the overexpression of ATF6β (392) ΔAD completely blocked the induction by ER stress of luciferase expressed from the GRP78 promoter (Figure 8B; compare the filled column in line 1 with that in line 3), demonstrating that ATF6β (392) ΔAD exhibits a dominant-

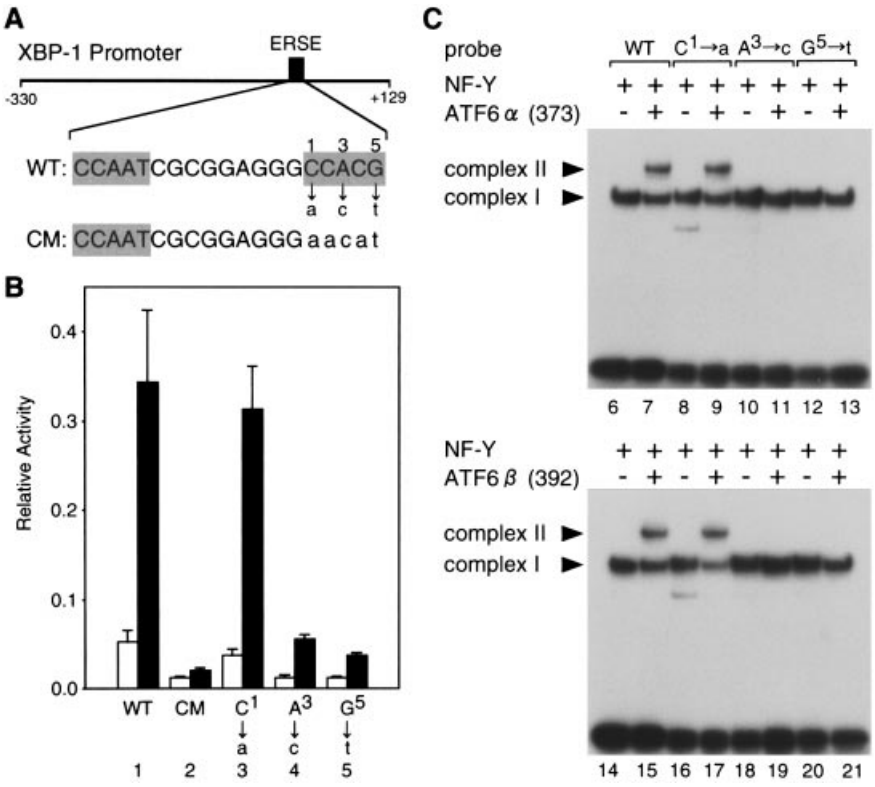

Figure 9 Effects of point mutations on ATF6 binding and transcription-inducing activities of ERSE

(**A**) Analysis of nucleotide sequences of wild-type and mutant forms of XBP-1-ERSE1. The structure of the human XBP-1 promoter is presented schematically. The numbers indicate locations from the transcription start site. The sequence of wild-type (WT) XBP-1-ERSE1 is shown and nucleotides matching the consensus ERSE are shaded. The CCACG part was mutated by multiple nucleotide replacement (referred to as CM) or point transversions as indicated. (**B**) Transcriptional response to ER stress of the XBP-1 promoter containing wild-type or mutant XBP-1-ERSE1. The XBP-1 promoter containing the wild-type (WT) or mutant version of XBP-1-ERSE1 as indicated was cloned immediately upstream of the firefly luciferase gene in the pGL3-Basic vector. The resulting plasmids were transiently introduced into HeLa cells with pRL-SV40 reference plasmid. Relative luciferase activities in transfected cells incubated for 16 h with (filled columns) or without (open columns) 2 μg/ml tunicamycin were determined; results are means $\pm$ S.D. for three independent experiments. (**C**) Binding of ATF6α and ATF6β to wild-type or mutant XBP-1-ERSE1. The wild-type (WT) or mutant version of XBP-1-ERSE1 was incubated after labelling with ^{32}P with (+) or without (−)ATF6α (373) or ATF6β (392), translated *in vitro*, in the presence of NF-Y. Protein–DNA complexes formed were analysed by EMSA. The positions of complexes I and II are indicated.

negative effect on the UPR, as with ATF6α (373) ΔAD reported previously [14].

To examine the effects on endogenous mRNA induction, we used HEK-293T cells, which seemed to exhibit a higher transfection efficiency than HeLa cells. GRP78 mRNA was induced approx. 6-fold by the treatment of HEK-293T cells with tunicamycin for 8 h (Figure 8C; compare lane 2 with lane 1). As expected from the results of the reporter assays in HeLa cells, overexpression in HEK-293T cells of ATF6β (392) constitutively enhanced the level of GRP78 mRNA (Figure 8C; compare lane 3 with lane 1), whereas overexpression of ATF6β (392) ΔAD blocked the induction of GRP78 mRNA by treatment with tunicamycin (Figure 8C; compare lane 6 with lane 5). The potent dominant-negative effect exhibited by overexpressed ATF6β (392) ΔAD that was observed at the level of endogenous UPR-target mRNA strongly supports the proposal that ATF6α/ATF6β or similar protein(s) are crucial transcriptional regulators of the mammalian UPR.

ATF6α and ATF6β are unable to bind to transcriptionally inactive point mutants of ERSE

We showed previously that the bZIP-type transcription factor XBP-1 is a target of the mammalian UPR and that its promoter region contains a single ERSE sequence (XBP-1-ERSE1) necessary and sufficient for the induction of XBP-1 by ER stress [14] [see Figure 9(A) for its schematic structure]. As shown in Figure 9(B), the wild-type XBP-1 promoter fused to the firefly luciferase gene responded to tunicamycin treatment by enhancing reporter expression 6-fold (lane 1). Mutation of the CCACG part of XBP-1-ERSE1 by multiple nucleotide replacement (the resulting mutant promoter being referred to as CM) completely inactivated the XBP-1 promoter (Figure 9B, lane 2). This observation is highly relevant to our findings that both ATF6α and ATF6β are unable to bind to ERSE-CM (Figure 7A) [14]. To substantiate the importance of ATF6α and ATF6β in the mammalian UPR, we examined how various point mutations of the CCACG moiety affect ATF6α/β binding and the transcription-inducing activities of ERSE. The first, third and fifth positions of the CCACG part of ERSE were mutated by transversion to create $C^1 \rightarrow a$, $A^3 \rightarrow c$ and $G^5 \rightarrow t$ mutants respectively. The $C^1 \rightarrow a$ mutation showed little effect (lane 3), whereas the $A^3 \rightarrow c$ and $G^5 \rightarrow t$ mutations greatly diminished the XBP-1 promoter activity (Figure 9B, lanes 4 and 5 respectively). It should be noted that the effects of these point mutations on the XBP-1-promoter activity are consistent with those on the transcriptional activity of ERSE transplanted to a heterologous SV40 promoter [9,14]. Most importantly, both ATF6α and ATF6β bound to the $C^1 \rightarrow$

a mutant (Figure 9C, lanes 9 and 17 respectively) as efficiently as to the wild type (lanes 7 and 15 respectively) but exhibited essentially no binding activity to either the $A^3 \rightarrow c$ mutant (lanes 11 and 19 respectively) or the $G^5 \rightarrow t$ mutant (lanes 13 and 21 respectively), revealing that the ATF6 binding activity of ERSE is highly correlated with the transcriptional activity of ERSE. Taking all these findings together, we concluded that the ER stress-induced proteolysis of ATF6α and ATF6β has a major role in the mammalian UPR.

DISCUSSION

The mammalian UPR is mediated by the *cis*-acting ERSE ($CCAATN_9CCACG$), the CCAAT part of which is the binding site for the general transcription factor NF-Y [10,13,14]. Because the transcription of ER chaperone genes is induced only when unfolded proteins have accumulated in the ER, the activity of *trans*-acting ERSF binding to ERSE must be tightly regulated. We proposed previously that ERSF is a heterologous protein complex composed of a constitutive component and an inducible component [12,14]. According to this model, the constitutive component binding to CCAAT (NF-Y) is involved in basal transcription, whereas the ER stress-inducible component binding to CCACG is responsible for the induction process in collaboration with the constitutive component. The bZIP protein ATF6α (the ATF6 gene product) has been best characterized as an inducible component [9,12,14]. We showed here that ATF6β (the G13/CREB-RP gene product) also functions as an inducible component of ERSF. Both ATF6α and ATF6β are synthesized as type II transmembrane glycoproteins anchored in the ER membrane and thus remain inactive under normal growth conditions (Figure 1). ATF6α and ATF6β are ubiquitously expressed (Figure 2). On the accumulation of unfolded proteins in the ER, both ATF6α and ATF6β are cleaved (Figure 3) and the resulting N-terminal fragments (p50ATF6α and p60ATF6β) liberated from the ER membrane are translocated into the nucleus; relocation of endogenous ATF6α and ATF6β was clearly seen in HeLa cells treated with dithiothreitol (Figure 5), which caused a rapid and extensive conversion of p90ATF6α into p50ATF6α as well as that of p110ATF6β into p60ATF6β (Figure 4). In the nucleus, both p50ATF6α and p60ATF6β activate the transcription of UPR-target genes via direct binding to the CCACG part of ERSE (Figure 7). Importantly, a mutant of p60ATF6β exhibited a strong dominant-negative effect on the UPR (Figure 8). Furthermore, the abilities of various ERSE-like sequences to bind ATF6α and ATF6β are well correlated with their ability to mediate transcriptional induction (Figure 9). On the basis of these results, we concluded that ATF6α and ATF6β are crucial transcriptional regulators of the mammalian UPR.

We found that the basic region is important for the nuclear localization of both p50ATF6α and p60ATF6β (Figure 6). This observation is consistent with the notion that nuclear proteins are generally tagged with NLS and that continuous or bipartite clustering of basic residues is characteristic of classical NLS [21]. Therefore p50ATF6α and p60ATF6β produced by ER stress-induced proteolysis are likely to be transported into the nucleus via the direct interaction between the NLS receptor, importin α, and the basic residues clustered in the basic region of ATF6α (RRQQRMIKNRESACQSRKKKKEY; single-letter amino acid codes) or that of ATF6β (KRQQRMIKNRESACQ-SRRKKKEY). Interestingly, ATF6α (330) and ATF6β (350), which lack the leucine zipper region, were accumulated in the nucleus (Figure 6), suggesting that the ATF6 monomer can translocate into the nucleus. ATF6α and ATF6β might form homodimers and/or heterodimers in the nucleus to exert transcriptional activator activity with the assistance of the recently identified nuclear protein BEF (bZIP enhancing factor) [22].

Roy and Lee [10] identified three proteins capable of binding to ERSE, namely NF-Y, which binds to the CCAAT part, YY1, a ubiquitous transcription factor that binds to the CCACG part, and an unknown protein that binds to the sequence GGC present between the CCAAT and CCACG parts. The importance of NF-Y is evident from both their and our findings; however, the role of the GGC-binding protein in the mammalian UPR remains unclear because the sequence GGC can be found only in GRP78-ERSE, as discussed previously [14]. It is also known that the DNA binding specificity of YY1 is not correlated with the transcriptional activity of ERSE, as seen from a point mutation of ERSE that changed CCACG to CCATG and inactivated it, but YY1 bound to this mutant ERSE with a higher affinity than it did to the wild-type ERSE [10]. In addition, it should be noted that these three ERSE-binding proteins were detected as three discrete bands when nuclear extracts of HeLa cells were analysed by EMSA, implying that their binding to ERSE is mutually exclusive and they cannot bind to the same DNA site. Li et al. [23] recently analysed the mechanism of activation of ATF6α by ER stress and proposed a model different from ours, namely that ATF6α activates the transcription of ER chaperone genes via protein–protein interactions, on the basis of the finding that ATF6α alone cannot bind to ERSE but can interact with YY1. However, we have demonstrated here that both ATF6α and ATF6β can directly bind to the CCACG part of ERSE when CCAAT is bound to NF-Y (Figure 7). Importantly, in marked contrast with the GGC-binding protein and YY1 mentioned above, ATF6α/β and NF-Y bind to ERSE simultaneously and can therefore co-operate to activate transcription. Furthermore, the DNA binding specificity of ATF6α/β was well correlated with the transcriptional activity of ERSE (Figure 9). These findings strongly favour the idea that ATF6α/β, and not YY1, is crucial as a transcription factor binding to the CCACG part of ERSE.

The next important issue to be resolved is the mechanism by which ER stress induces the proteolysis of ATF6α and ATF6β. It is widely thought that the presence of unfolded proteins in the ER is somehow sensed by the luminal domain of Ire1p/Ern1p, a type I transmembrane glycoprotein localized in the ER, leading to activation of its cytoplasmic kinase/endonuclease domain via oligomerization and autophosphorylation [7,8]. Ire1p was originally isolated by genetic screening in *Saccharomyces cerevisiae*; disruption of the *IRE1* locus inactivated the yeast UPR [5,6]. Mammalian cells were recently found to express two Ire1p homologues in the ER, designated IRE1α and IRE1β [24–26]. Overexpression of IRE1α or IRE1β activated the mammalian UPR constitutively, whereas overexpression of mutant IRE1α or IRE1β lacking the cytosolic effector domain exhibited a dominant-negative effect on the UPR [24,25], indicating the importance of IRE1α and IRE1β in signalling from the ER. Recent studies have shown that chaperone protein BiP/GRP78 is directly involved in the activation of IRE1 [27]. Unexpectedly, however, UPR remained intact in mouse fibroblasts lacking IRE1α [28] or lacking both IRE1α and IRE1β [8], suggesting that proteolysis of ATF6α or ATF6β could occur in the absence of IRE1α and IRE1β. This raised the intriguing possibility that ATF6α or ATF6β itself could act as a sensor for protein folding status in the ER; under the conditions of ER stress, neither ATF6α nor ATF6β would be able to fold properly in the lumen of the ER. In this connection, it is noteworthy that the extent of ATF6α processing is well correlated with the strength of ER stress; the amounts of p50ATF6α produced were dependent on the dose of dithiothreitol added (Figure 4), which can cause

malfolding of ATF6α directly owing to the presence of two cysteine residues in its luminal domain. Unfolded ATF6α and ATF6β might therefore be preferentially subjected to proteolysis. We are currently testing this hypothesis.

We thank Masako Nakayama, Seiji Takahara and Tomoko Yoshifusa for technical assistance. This work was supported in part by Research for the Future Program of the Japan Society for the Promotion of Science.

REFERENCES

1 Gething, M. J. and Sambrook, J. (1992) Protein folding in the cell. Nature (London) **355**, 33–45
2 Helenius, A., Marquardt, T. and Braakman, I. (1992) The endoplasmic reticulum as a protein folding compartment. Trends Cell Biol. **2**, 227–231
3 Lee, A. S. (1987) Coordinated regulation of a set of genes by glucose and calcium ionophores in mammalian cells. Trends Biochem. Sci. **12**, 20–23
4 Kozutsumi, Y., Segal, M., Normington, K., Gething, M. J. and Sambrook, J. (1988) The presence of malfolded proteins in the endoplasmic reticulum signals the induction of glucose-regulated proteins. Nature (London) **332**, 462–464
5 Cox, J. S., Shamu, C. E. and Walter, P. (1993) Transcriptional induction of genes encoding endoplasmic reticulum resident proteins requires a transmembrane protein kinase. Cell **73**, 1197–1206
6 Mori, K., Ma, W., Gething, M. J. and Sambrook, J. (1993) A transmembrane protein with a cdc2+/CDC28-related kinase activity is required for signaling from the ER to the nucleus. Cell **74**, 743–756
7 Kaufman, R. J. (1999) Stress signaling from the lumen of the endoplasmic reticulum: coordination of gene transcriptional and translational controls. Genes Dev. **13**, 1211–1233
8 Mori, K. (2000) Tripartite management of unfolded proteins in the endoplasmic reticulum. Cell **101**, 451–454
9 Yoshida, H., Haze, K., Yanagi, H., Yura, T. and Mori, K. (1998) Identification of the *cis*-acting endoplasmic reticulum stress response element responsible for transcriptional induction of mammalian glucose-regulated proteins; involvement of basic-leucine zipper transcription factors. J. Biol. Chem. **273**, 33741–33749
10 Roy, B. and Lee, A. S. (1999) The mammalian endoplasmic reticulum stress response element consists of an evolutionarily conserved tripartite structure and interacts with a novel stress-inducible complex. Nucleic Acids Res. **27**, 1437–1443
11 Roy, B., Li, W. W. and Lee, A. S. (1996) Calcium-sensitive transcriptional activation of the proximal CCAAT regulatory element of the *grp78*/BiP promoter by the human nuclear factor CBF/NF-Y. J. Biol. Chem. **271**, 28995–29002
12 Haze, K., Yoshida, H., Yanagi, H., Yura, T. and Mori, K. (1999) Mammalian transcription factor ATF6 is synthesized as a transmembrane protein and activated by proteolysis in response to endoplasmic reticulum stress. Mol. Biol. Cell **10**, 3787–3799
13 Li, W. W., Sistonen, L., Morimoto, R. I. and Lee, A. S. (1994) Stress induction of the mammalian GRP78/BiP protein gene: in vivo genomic footprinting and identification of p70CORE from human nuclear extract as a DNA-binding component specific to the stress regulatory element. Mol. Cell. Biol. **14**, 5533–5546
14 Yoshida, H., Okada, T., Haze, K., Yanagi, H., Yura, T. and Mori, K. (2000) ATF6 activated by proteolysis directly binds in the presence of NF-Y (CBF) to the *cis*-acting element responsible for the mammalian unfolded protein response. Mol. Cell. Biol. **20**, 6755–6767
15 Zhu, C., Johansen, F. E. and Prywes, R. (1997) Interaction of ATF6 and serum response factor. Mol. Cell. Biol. **17**, 4957–4966
16 Khanna, A. and Campbell, R. D. (1996) The gene G13 in the class III region of the human MHC encodes a potential DNA-binding protein. Biochem. J. **319**, 81–89
17 Min, J., Shukla, H., Kozono, H., Bronson, S. K., Weissman, S. M. and Chaplin, D. D. (1995) A novel Creb family gene telomeric of HLA-DRA in the HLA complex. Genomics **30**, 149–156
18 Sambrook, J., Fritsch, E. F. and Maniatis, T. (1989) Molecular Cloning: A Laboratory Manual, 2nd edn, Cold Spring Harbor Laboratory, Cold Spring Harbor, NY
19 Tanaka, M. and Herr, W. (1990) Differential transcriptional activation by Oct-1 and Oct-2: interdependent activation domains induce Oct-2 phosphorylation. Cell **60**, 375–386
20 Li, W. W., Alexandre, S., Cao, X. and Lee, A. S. (1993) Transactivation of the grp78 promoter by Ca^{2+} depletion. A comparative analysis with A23187 and the endoplasmic reticulum Ca^{2+}-ATPase inhibitor thapsigargin. J. Biol. Chem. **268**, 12003–12009
21 Dingwall, C. and Laskey, R. A. (1991) Nuclear targeting sequences–a consensus? Trends Biochem. Sci. **16**, 478–481
22 Virbasius, C. M. A., Wagner, S. and Green, M. R. (1999) A human nuclear-localized chaperone that regulates dimerization, DNA binding, and transcriptional activity of bZIP proteins. Mol. Cell **4**, 219–228
23 Li, M., Baumeister, P., Roy, B., Phan, T., Foti, D., Luo, S. and Lee, A. S. (2000) ATF6 as a transcription activator of the endoplasmic reticulum stress element: thapsigargin stress-induced changes and synergistic interactions with NF-Y and YY1. Mol. Cell. Biol. **20**, 5096–5106
24 Tirasophon, W., Welihinda, A. A. and Kaufman, R. J. (1998) A stress response pathway from the endoplasmic reticulum to the nucleus requires a novel bifunctional protein kinase/endoribonuclease (Ire1p) in mammalian cells. Genes Dev. **12**, 1812–1824
25 Wang, X.-Z., Harding, H. P., Zhang, Y., Jolicoeur, E. M., Kuroda, M. and Ron, D. (1998) Cloning of mammalian Ire1 reveals diversity in the ER stress responses. EMBO J. **17**, 5708–5717
26 Niwa, M., Sidrauski, C., Kaufman, R. J. and Walter, P. (1999) A role for presenilin-1 in nuclear accumulation of Ire1 fragments and induction of the mammalian unfolded protein response. Cell **99**, 691–702
27 Bertolotti, A., Zhang, Y., Hendershot, L. M., Harding, H. P. and Ron, D. (2000) Dynamic interaction of BiP and ER stress transducers in the unfolded-protein response. Nat. Cell Biol. **2**, 326–332
28 Urano, F., Wang, X., Bertolotti, A., Zhang, Y., Chung, P., Harding, H. P. and Ron, D. (2000) Coupling of stress in the ER to activation of JNK protein kinases by transmembrane protein kinase IRE1. Science **287**, 664–666
29 Kyte, J. and Doolittle, R. F. (1982) A simple method for displaying the hydropathic character of a protein. J. Mol. Biol. **157**, 105–132

Received 28 September 2000/13 December 2000; accepted 26 January 2001